Electronic Supplementary Material (ESI) for Environmental Science: Nano.

Supplementary information

Electrospray interfacial polymerization for a loose NF membrane: Super-selective dye separation in saline dye wastewater treatment

Yesol Kang[a], Jaewon Jang[a], Yunho Lee[a], and In S. Kim[a,*]

[a]School of Earth Sciences and Environmental Engineering (SESE), Gwangju Institute of Science and Technology (GIST), 123 Cheomdangwagi-ro, Buk-gu, Gwangju 61005, Republic of Korea

* Corresponding author: Tel: +82-62-715-2436, e-mail: iskim@gist.ac.kr

Table S1. Characteristics of the dye molecules used in this study

Dye name	Molecular formula	Molecular structure	Molecular weight (g mol^{-1})	Nature	UV adsorption (nm)
Evans blue	$C_{34}H_{24}N_6Na_4O_{14}S_4$	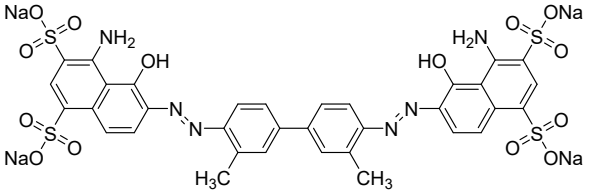	960.8	Negative	606
Congo red	$C_{32}H_{22}N_6Na_2O_6S_2$	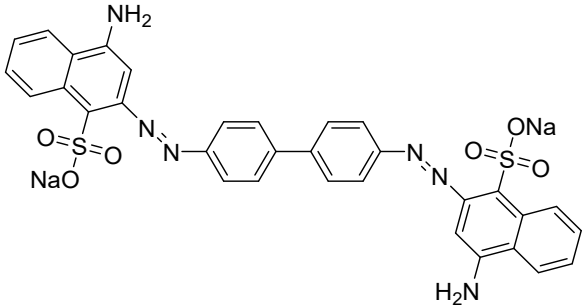	696.7	Negative	495
Methyl orange	$C_{14}H_{14}N_3NaO_3S$	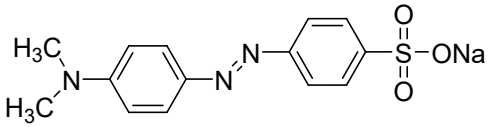	327.3	Negative	461

Table S2. C 1s, O 1s, and S 2p core-level XPS spectra of GO, and SGO.

	GO	SGO
C 1s	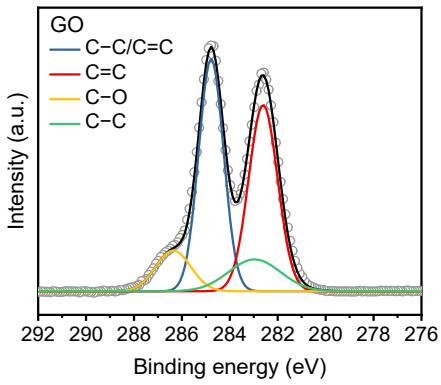	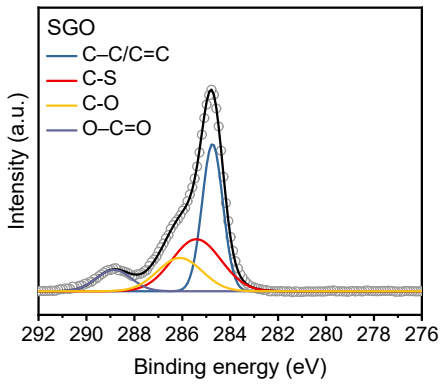
O 1s	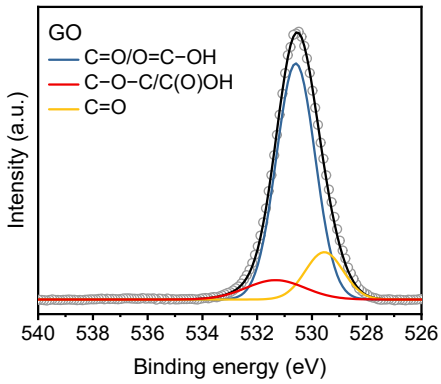	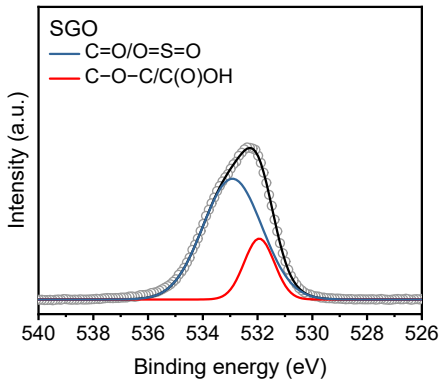
S 2p	N/A	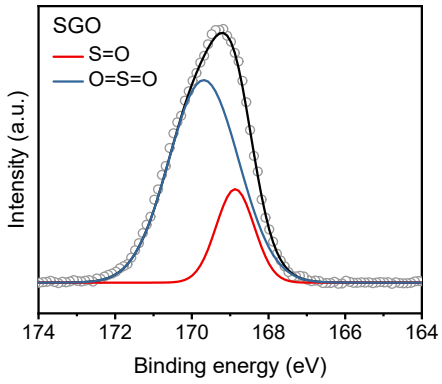

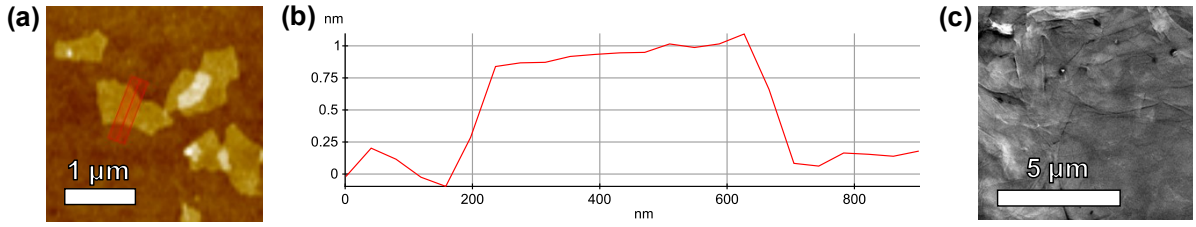

Fig. S1. (a) A tapping mode AFM image of SGO sheets and (b) the height profile of the AFM image. (c) The SEM image of SGO sheet at a magnification of ×10k.

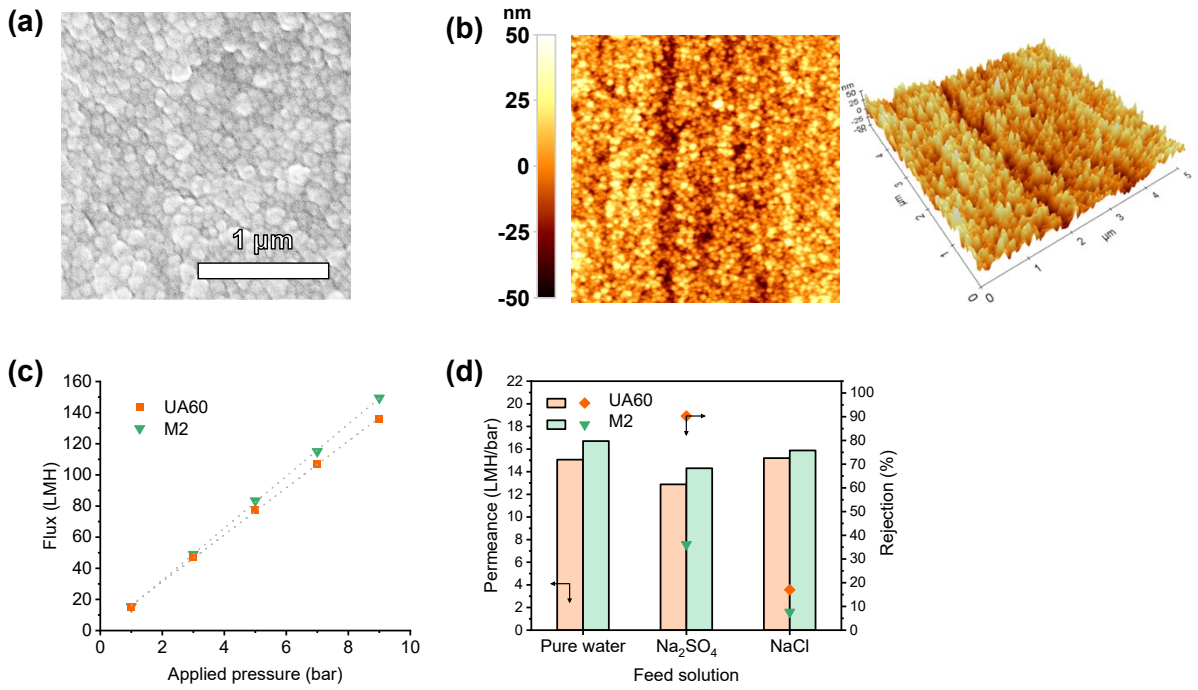

Fig. S2. (a) SEM surface images, (b) AFM surface scanning images of UA60 membrane, (c) pure water flux depending on the applied pressure (UA60 to 15.1 LMH bar^{-1}), and (d) permeance and salt rejection comparison of UA60 and M2 under operating pressure at 5 bar.

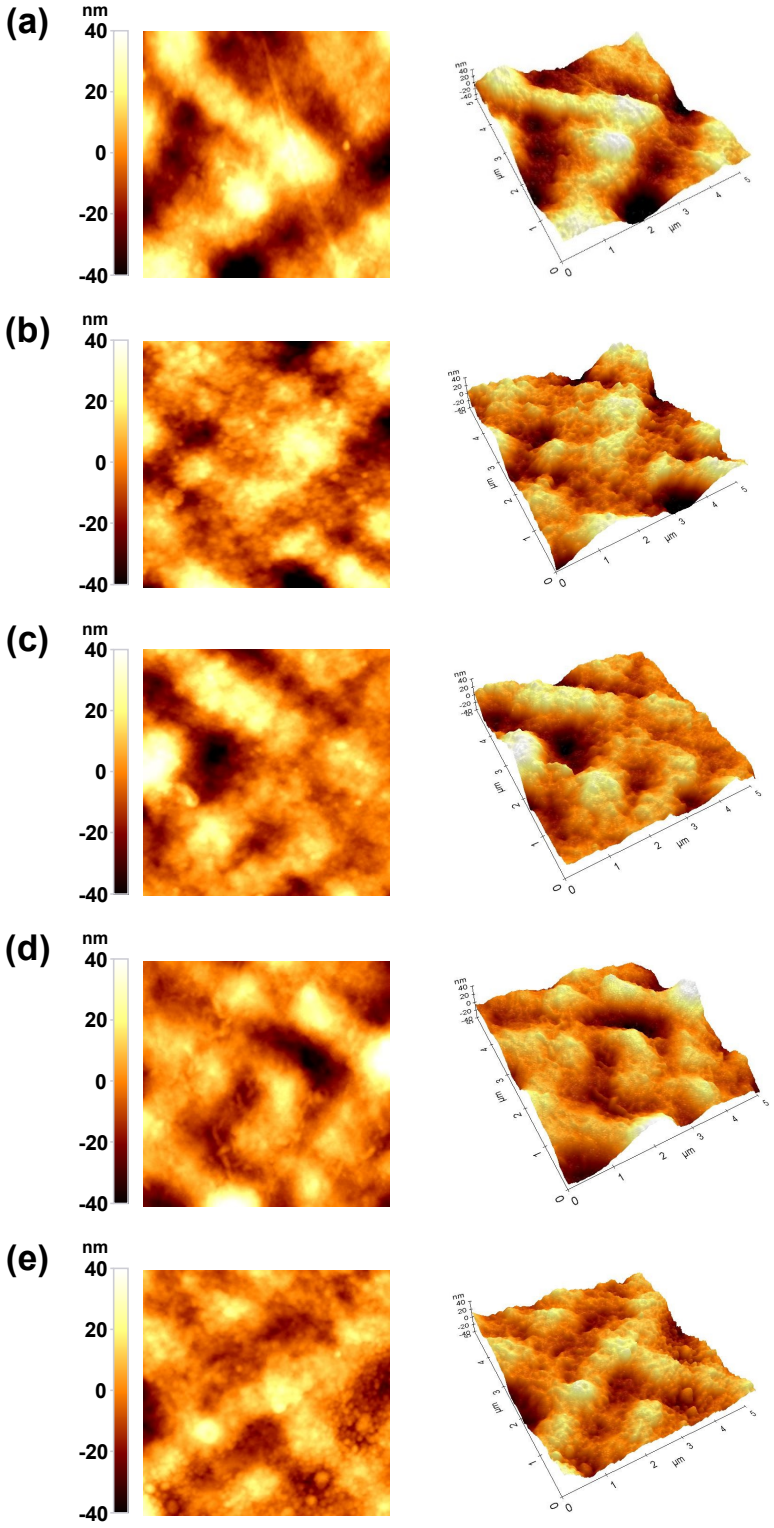

Fig. S3. Surface AFM images of SGO contained membranes: (a) M0, (b) M1, (c) M1.5, (d) M2, and (e) M3.

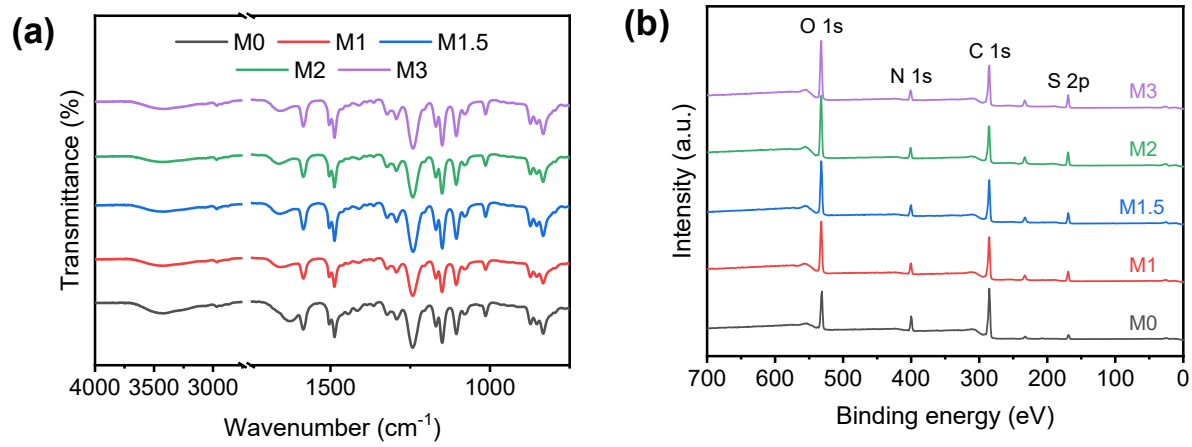

Fig. S4. (a) ATR-FTIR and (b) XPS spectra of the prepared membranes.

Table S3. The atomic percentage of element (%) obtained from XPS of membranes

Membrane	Elemental ratio (%)			
	C 1s	N 1s	O 1s	S 2p
M0	66.4	10.9	20.1	2.6
M1	58.8	8.4	27.2	5.6
M1.5	56.1	8.9	28.8	6.2
M2	52.1	7.9	32.2	7.8
M3	54.7	7.7	30.3	7.3

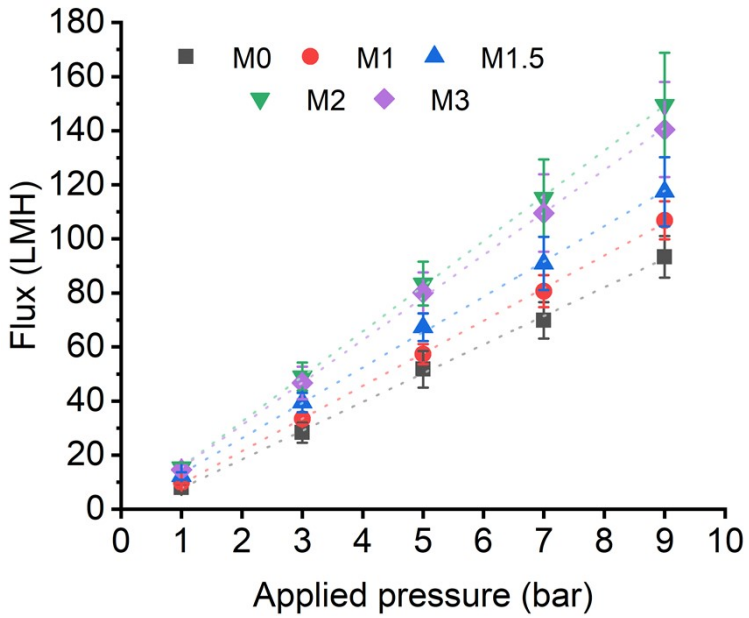

Fig. S5. Membrane flux differences depending on the applied pressure and membrane; PWP values of membranes are 11.0 ± 0.8, 12.1 ± 0.9, 13.1 ± 1.5, 16.7 ± 2.2, and 15.7 ± 2.0 LMH bar^{-1}, corresponding to M0, M1, M1.5, M2, and M3.

Table S4. Comparison of the permeance, dye rejection, and salt rejection.

Membrane	Permeance (LMH bar^{-1})	Dye	Dye rejection (%)	Salt	Salt rejection (%)	Ref.
GO-PCS	13.2	Direct black 38	99.7	NaCl	56.8	1
				Na_2SO_4	87.8	
(PEI-modified GO)/PAA/PVA/GA	0.84	Congo red	99.5	NaCl	37.8	2
		Methyl blue	99.3			
GOQDs-1	11.7	Congo red	99.8	NaCl	17.2	3
		Methyl blue	97.6			
GO(120) NFM	11.1	Methyl blue	98.88	NaCl	27.86	4
GO@PAN	5	Congo red	99.9	NaCl	9.8	5
				Na_2SO_4	56.7	
PDA-rGOC2	16.8	Congo red	99.6	NaCl	43.2	6
PAN/GO	5.5	Acid red 18	99.8	NaCl	10.9	7
		Methyl blue	100	$MgCl_2$	11.3	
PES/Metformin/GO/Fe_3O_4	9.02	Direct red 16	99	NaCl	15	8
HNTs-poly(NASS)/PES	10.8	Reactive black 5	85.5	NaCl	6.9	9
				Na_2SO_4	12	
Polypiperazine-amide NF	7.0	Reactive black 5	99.3	NaCl	66.7	10
				Na_2SO_4	98.9	
UA60	15.1	EB	99.8	NaCl	17.0	This work
		CR	99.5	Na_2SO_4	90.3	
M0	11.0	EB	99.5	NaCl	24.5	
		CR	99.9	Na_2SO_4	52.8	
M2	16.7	EB	99.6	NaCl	7.7	
		CR	99.8	Na_2SO_4	36.1	

References

1 Y. Song, Y. Sun, M. Chen, P. Huang, T. Li, X. Zhang and K. Jiang, Efficient removal and fouling-resistant of anionic dyes by nanofiltration membrane with phosphorylated chitosan modified graphene oxide nanosheets incorporated selective layer, *J. Water Process Eng.*, 2020, **34**, 101086.
2 N. Wang, S. Ji, G. Zhang, J. Li and L. Wang, Self-assembly of graphene oxide and polyelectrolyte complex nanohybrid membranes for nanofiltration and pervaporation, *Chem. Eng. J.*, 2012, **213**, 318–329.
3 C. Zhang, K. Wei, W. Zhang, Y. Bai, Y. Sun and J. Gu, Graphene Oxide Quantum Dots Incorporated into a Thin Film Nanocomposite Membrane with High Flux and Antifouling Properties for Low-Pressure Nanofiltration, *ACS Appl. Mater. Interfaces*, 2017, **9**, 11082–11094.
4 L. Chen, J. H. Moon, X. Ma, L. Zhang, Q. Chen, L. Chen, R. Peng, P. Si, J. Feng, Y. Li, J. Lou and L. Ci, High performance graphene oxide nanofiltration membrane prepared by electrospraying for wastewater purification, *Carbon*, 2018, **130**, 487–494.
5 J. Wang, P. Zhang, B. Liang, Y. Liu, T. Xu, L. Wang, B. Cao and K. Pan, Graphene Oxide as an Effective Barrier on a Porous Nanofibrous Membrane for Water Treatment, *ACS Appl. Mater. Interfaces*, 2016, **8**, 6211–6218.
6 J. Zhu, J. Wang, A. A. Uliana, M. Tian, Y. Zhang, Y. Zhang, A. Volodin, K. Simoens, S. Yuan, J. Li, J. Lin, K. Bernaerts and B. Van Der Bruggen, Mussel-Inspired Architecture of High-Flux Loose Nanofiltration Membrane Functionalized with Antibacterial Reduced Graphene Oxide-Copper Nanocomposites, *ACS Appl. Mater. Interfaces*, 2017, **9**, 28990–29001.
7 Z. Qiu, X. Ji and C. He, Fabrication of a loose nanofiltration candidate from Polyacrylonitrile/Graphene oxide hybrid membrane via thermally induced phase separation, *J. Hazard. Mater.*, 2018, **360**, 122–131.
8 G. Abdi, A. Alizadeh, S. Zinadini and G. Moradi, Removal of dye and heavy metal ion using a novel synthetic polyethersulfone nanofiltration membrane modified by magnetic graphene oxide/metformin hybrid, *J. Membr. Sci.*, 2018, **552**, 326–335.
9 J. Zhu, N. Guo, Y. Zhang, L. Yu and J. Liu, Preparation and characterization of negatively charged PES nanofiltration membrane by blending with halloysite nanotubes grafted with poly (sodium 4-styrenesulfonate) via surface-initiated ATRP, *J. Membr. Sci.*, 2014, **465**, 91–99.
10 S. Yu, M. Liu, M. Ma, M. Qi, Z. Lü and C. Gao, Impacts of membrane properties on reactive dye removal from dye/salt mixtures by asymmetric cellulose acetate and composite polyamide nanofiltration membranes, *J. Membr. Sci.*, 2010, **350**, 83–91.

Table S5. BSA adsorption capability, and FRR of the fabricated membranes

Membrane	BSA adsorption capability ($\mu g\ cm^{-2}$)	FRR (%)	
		2nd cycle	3rd cycle
M0	33.9 ± 3.3	88.5	87.9
M2	10.5 ± 6.1	96.4	97.9